



MULTI-CRITERIA DESIGN OF SEISMIC PROTECTIVE DEVICES BASED ON LIFE-CYCLE OBJECTIVES AND RISK AVERSION PRINCIPLES

I. Gidaris⁽¹⁾, A. A. Taflanidis⁽²⁾, G. P. Mavroeidis⁽³⁾

⁽¹⁾ Postdoctoral Scholar, Rice University, ig11@rice.edu

⁽²⁾ Associate Professor, University of Notre Dame, a.taflanidis@nd.edu

⁽³⁾ Assistant Professor, University of Notre Dame, g.mavroeidis@nd.edu

Abstract

Significant advances have been established in the last decade in seismic-risk decision management through development of assessment and design methodologies based on detailed socio-economic metrics quantifying performance, such as casualties, repair costs and downtime. The associated design approaches are particularly relevant for supplemental seismic protective devices, for which a comprehensive socio-economic justification is frequently necessary to promote adoption. A probabilistic framework for the cost-effective design of such devices considering multiple criteria related to their life-cycle performance is presented in this contribution, focusing on application to fluid viscous dampers. The framework is based on nonlinear time-history analysis for describing structural behavior, an assembly-based vulnerability approach for quantifying earthquake losses, and on characterization of the earthquake hazard through stochastic ground motion modeling. In this setting life-cycle performance is described through the expected value of some properly defined risk consequence measure over the space of the uncertain parameters (i.e. random variables) for the structural system and the seismic hazard.

The main objective considered for quantifying life-cycle performance is the expected life-cycle cost, composed of the upfront protective system cost and the present value of future earthquake losses. To offer greater versatility and incorporate risk-aversion attitudes in the decision making process, additional objectives are examined, corresponding to consequences, such as repair cost or downtime, with specific probability of exceedance over the lifetime of the structure. This explicitly accounts for low likelihood but high impact events, and ultimately leads to a multi-criteria design setting, representing competing objectives to the life-cycle cost and allowing to incorporate resilience and sustainability considerations in the design process. To facilitate adoption of complex numerical and probability models, a computational framework relying on kriging surrogate modeling is established for performing the resultant multi-objective optimization. The surrogate model is formulated in an augmented input space, composed of both the uncertain model parameters and the design variables (controllable device parameters) and therefore is used to simultaneously support both the uncertainty propagation (calculation of risk integrals for the life-cycle performance) and the design optimization. As an illustrative example the retrofitting of a three-story building with nonlinear fluid viscous dampers is examined.

Keywords: Life-cycle cost; multi-objective design; kriging metamodeling; fluid viscous dampers; risk-averse design



1. Introduction

In the last decades significant advances have been established in seismic-risk decision management through development of assessment and design methodologies based on detailed socio-economic metrics quantifying performance, such as casualties, repair costs and downtime [1]. Within this context, the life-cycle cost analysis of structures has been becoming increasingly popular. This analysis considers in the decision making the contributions from the initial (upfront) cost as well as the expected direct and indirect losses due to future seismic events, and has motivated researchers to look into the life-cycle cost-based assessment/design of structures [2], especially in the context of design of supplemental seismic protective devices [3, 4]. In the latter case life-cycle analysis can provide a comprehensive justification for the proposed seismic upgrades, which constitutes a necessary step for adoption of such alternative earthquake-protective measures.

The aforementioned research efforts for life-cycle design of supplemental protective devices have focused, though, on adoption of a single objective, mainly the total life-cycle cost. Studies that have considered multiple criteria are limited [5, 6] and have examined only simplified metrics for representing the competing objectives. It is becoming, though, increasingly evident [7, 8], that seismic-risk decision management can greatly benefit from consideration of advanced metrics for quantifying life-cycle performance, especially criteria that can describe risk-averse attitudes. Of course, adoption of such metrics comes at the expense of an increased computational burden for their accurate quantification/calculation and for supporting the associated design optimization. This paper presents a computationally efficient, multi-objective design framework that can facilitate the adoption of enhanced life-cycle performance criteria for the competing objectives. Though the framework is general, the focus of the application is on fluid viscous dampers which represent a popular seismic upgrade strategy.

The approach is based on nonlinear time-history analysis for describing structural behavior, an assembly-based vulnerability approach for quantifying losses and on characterization of the hazard through stochastic ground motion modeling. The main objective considered for quantifying life-cycle performance is the expected life-cycle cost, composed of the upfront protective system cost and the present value of future earthquake losses. To offer greater versatility and incorporate risk-aversion attitudes in the decision making process, additional objectives are examined, corresponding to consequences, such as repair cost or downtime, with specific probability of exceedance over the lifetime of the structure. This explicitly accounts for low likelihood but high impact events, and ultimately leads to a multi-criteria design setting, representing competing objectives to the life-cycle cost while allowing to incorporate resilience and sustainability considerations in the design process. To facilitate adoption of complex numerical and probability models, a computational framework relying on kriging surrogate modeling is described for performing the resultant risk assessment and multi-objective optimization.

2. Seismic risk quantification and life-cycle performance characterization

2.1 Seismic risk quantification

The probabilistic framework from [4] is adopted to describe seismic risk. The framework, shown in Fig. 1, is based on adoption of appropriate models for the seismic excitation (hazard analysis), structural system (structural analysis) and loss evaluation (damage and loss analysis), and on assigning appropriate probability distributions to the parameters that are considered as uncertain in these different models. The combination of the first two models within this augmented model description of Fig. 1 provides the structural response, denoted \mathbf{z} herein, and this is established in terms of nonlinear time-history analysis and ultimately approximated through a kriging surrogate model as will be detailed later. The loss evaluation model quantifies, then, earthquake performance in socio-economic terms based on that response through an assembly-based vulnerability approach. Seismic excitation (acceleration time-histories) is described through a stochastic ground motion modeling approach, established by describing separately and then combining the broadband (high-frequency) and near-fault (long-period) components of the excitation. The first component is represented through a point source stochastic model [9] that entails modulation of a high-dimensional white noise sequence $\mathbf{w} \in \mathcal{W}$, through functions that address the frequency and time-domain characteristics of the excitation. Near-fault characteristics are incorporated through the velocity pulse model proposed by Mavroeidis and Papageorgiou [10].

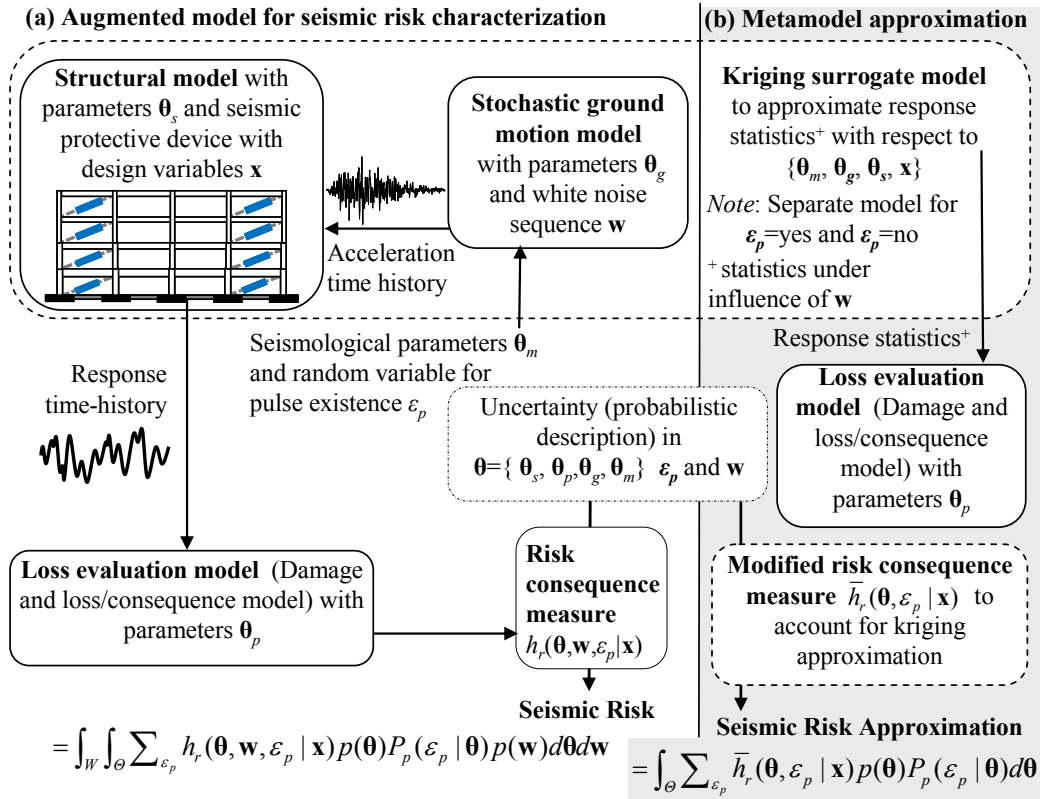


Fig. 1 – (a) Augmented model for life-cycle performance (seismic risk) quantification and (b) its approximation through a kriging surrogate model.

To formalize this modeling let θ lying in $\Theta \subset \mathcal{R}^{n_\theta}$, denote the augmented vector of continuous uncertain model parameters with probability density functions (PDFs) denoted as $p(\theta)$, where Θ denotes the space of possible parameter-values. This vector includes all the different parameters (either seismological, or structural or ground motion related) that are considered as uncertain. The random characteristics in the model description involve, additionally, the high-dimensional white noise sequence $\mathbf{w} \in W$ utilized in the stochastic ground motion model, with probability distribution function $p(\mathbf{w})$, and a discrete random variable ε_p with binary outcome {yes, no} to describe the pulse existence, with probability model $P(\varepsilon_p | \theta)$ [$\varepsilon_p = \text{yes}$ means that excitation combines both the broadband and near-fault components, whereas for $\varepsilon_p = \text{no}$ only broadband component exists]. Also, let the vector of controllable parameters for the seismic protective device (its properties that can be adjusted), referred to herein as *design variables*, be $\mathbf{x} \in X \subset \mathcal{R}^{n_x}$, where X denotes the admissible design space.

For a specific design configuration \mathbf{x} the risk consequence measure, representing the utility of the response from a decision-theoretic point of view, is given by $h_r(\theta, \mathbf{w}, \varepsilon_p | \mathbf{x})$. Each consequence measure $h_r(\cdot)$ is related to (i) the earthquake performance/losses that can be calculated based on the estimated response of the structure \mathbf{z} (losses for a specific event), as well as to (ii) the rate of occurrence of earthquakes (incorporation of the probability of seismic events occurring). Seismic risk, $H_r(\mathbf{x})$, is then described through

$$H_r(\mathbf{x}) = \int_W \int_{\Theta} \sum_{\varepsilon_p} h_r(\theta, \mathbf{w}, \varepsilon_p | \mathbf{x}) p(\theta) P_p(\varepsilon_p | \theta) p(\mathbf{w}) d\theta d\mathbf{w} \quad (1)$$

2.2 Life-cycle performance metrics needed in the multi-objective design

The main life-cycle performance metric needed in the design formulation is the total life-cycle cost $C(\mathbf{x})$, provided by adding the initial (upfront) cost $C_i(\mathbf{x})$, which is directly a function of the characteristics of the protective system, and the cost due to earthquake losses over the life-cycle of the structure $C_l(\mathbf{x})$, $C(\mathbf{x}) = C_i(\mathbf{x}) + C_l(\mathbf{x})$. For the latter only direct losses due to repair cost are considered here, though the framework can be extended, as also demonstrated in [1], to address other loss-components. For a Poisson assumption for occurrence of earthquakes, $C_l(\mathbf{x})$ is given by integral (1) with risk consequence measure definition [1]



$$h_r(\boldsymbol{\theta}, \mathbf{w}, \varepsilon_p | \mathbf{x}) = L_l(\boldsymbol{\theta}, \mathbf{w}, \varepsilon_p | \mathbf{x}) v t_{life} [(1 - e^{-r_d t_{life}}) / r_d t_{life}] \quad (2)$$

where r_d is the discount rate, t_{life} is the life cycle considered and $L_l(\boldsymbol{\theta}, \mathbf{w}, \varepsilon_p | \mathbf{x})$ is the cost given the occurrence of an earthquake event. For estimating the latter an assembly-based vulnerability approach is adopted: the elements of the structure are grouped into damageable assemblies and different damage states are designated for each assembly. A fragility function and repair cost estimates are established for each damage state, with the former conditional on some response quantity of interest z_k (representing the engineering demand parameter –EDP– for the assembly). The fundamental component of this approach is the fragility function for which a lognormal distribution is typically adopted. This leads to the following probability for the k^{th} damageable assembly exceeding its j^{th} state

$$P[d_{kj} | z_k] = \Phi[\ln(z_k / \beta_{kj}) / \sigma_{kj}] \quad (3)$$

where Φ stands for the standard Gaussian cumulative distribution function (CDF), d_{kj} represents the j^{th} damage state for the k^{th} assembly, β_{kj} is the median threshold for d_{kj} and σ_{kj} the associated logarithmic standard deviation. If n_{dk} is the number of the different damage states for the k^{th} assembly, n_{as} the number of total assemblies considered, and C_{kj} the repair cost associated with d_{kj} , the seismic losses are given by

$$L_l(\boldsymbol{\theta}, \mathbf{w}, \varepsilon_p | \mathbf{x}) = \sum_{k=1}^{n_{as}} \sum_{j=1}^{n_{dk}} P_e[d_{kj} | z_k] C_{kj} \quad (4)$$

$$P_e[d_{kj} | z_k] = P[d_{kj} | z_k] - P[d_{k(j+1)} | z_k] ; P_e[d_{kn_{dk}} | z_k] = P[d_{kn_{dk}} | z_k]$$

The upfront cost, $C_l(\mathbf{x})$, now depends on the details of the specific system examined. For a variety of protective systems this cost can be related to the capacity [11] required under some chosen design event. For fluid viscous dampers, which will be the application examined later, the forces exerted by the dissipative device are a function of the relative velocity across the end points of the damper v_D and the upfront cost can be correlated to a reference ultimate force capacity F_{Du} under the maximum credible earthquake [4]. This ultimately entails calculation of the reference velocity $v_{ref}(\mathbf{x})$ with certain probability of exceedance over the lifetime of the structure. Under the established seismic hazard description the latter probability is given by

$$P[v_D > v_{ref}(\mathbf{x}) | \mathbf{x}, t_{life}] = 1 - \exp^{-t_{life} v \cdot P[v_D > v_{ref}(\mathbf{x}) | \mathbf{x}, \text{seismic event}]} \quad (5)$$

where $P[v_D > v_{ref}(\mathbf{x}) | \mathbf{x}, \text{seismic event}]$ is the mean rate (probability) of exceeding the reference velocity given an event occurring, and is expressed through the generic integral (1) for a definition of the risk consequence measure $h_r(\boldsymbol{\theta}, \mathbf{w}, \varepsilon_p | \mathbf{x}) = I_{v_{ref}}(\boldsymbol{\theta}, \mathbf{w}, \varepsilon_p | \mathbf{x})$ corresponding to an indicator function, which is one if $v_D > v_{ref}(\mathbf{x})$ and zero if $v_D \leq v_{ref}(\mathbf{x})$.

An additional metric that will be utilized in the multi-objective design formulation is the seismic event consequences, such as repair cost or repair time, with specific probability of being exceeded over the lifetime of the structure. For the repair cost L_l , described by (4) for a specific seismic event, the probability of exceeding a targeted threshold $C_{thresh}(\mathbf{x})$ is given by an Equation similar to (5) simply by replacing the $v_D > v_{ref}(\mathbf{x})$ argument with $L_l > C_{thresh}(\mathbf{x})$. This entails calculation of the probability $P[L_l > C_{thresh}(\mathbf{x}) | \mathbf{x}, t_{life}]$ of exceeding the repair threshold for a given seismic event which is given by the generic risk integral (1) with risk consequence measure $h_r(\boldsymbol{\theta}, \mathbf{w}, \varepsilon_p | \mathbf{x}) = I_C(\boldsymbol{\theta}, \mathbf{w}, \varepsilon_p | \mathbf{x})$ corresponding to an indicator function, being one if $L_l(\boldsymbol{\theta}, \mathbf{w}, \varepsilon_p | \mathbf{x}) > C_{thresh}(\mathbf{x})$ and zero if not. Similar approach holds for the repair time R_T and its corresponding threshold $R_{thresh}(\mathbf{x})$ with the only difference that the risk consequence measure needs to be substituted by the corresponding indicator function related to the repair time for specific seismic event $R_T(\boldsymbol{\theta}, \mathbf{w}, \varepsilon_p | \mathbf{x})$ exceeding R_{thresh} or not. The repair time $R_T(\boldsymbol{\theta}, \mathbf{w}, \varepsilon_p | \mathbf{x})$ is calculated through the assembly-based vulnerability approach used for $L_l(\boldsymbol{\theta}, \mathbf{w}, \varepsilon_p | \mathbf{x})$, simply by assigning a repair time R_{kj} for each damage state in (4) rather than a repair cost C_{kj} [12].

3. Multi-objective design formulation

The fundamental metric that needs to be examined for design based on life-cycle criteria is the mean total life cycle cost $C(\mathbf{x})$ [13]. Consideration of only this performance objective facilitates a “risk-neutral” design, which assumes that preference is assessed only through quantities that can be monetized. In reality, though, engineers



and stakeholders have to take into account social risk perceptions that inevitably lead to more conservative designs (*risk aversion*) [7, 8]. Motivated by this concept the additional metrics for the multi-criteria design proposed here correspond to performance quantities, such as repair costs or repair time, with specific probability of exceedance over the life-cycle of the structure. Appropriate selection of this probability-level allows consideration of low-likelihood events within the design, whereas different selection of the aforementioned performance quantities supports stakeholder's preference towards them and could potentially facilitate further integration of concepts related to resiliency or sustainability. Adoption of these types of enhanced metrics supports the goal of providing to decision makers a spectrum of design solutions related to different attitudes towards risk, since minimization of expected life-cycle cost represents “*risk-neutral*” designs, whereas minimization of the latter type of metrics represents “*risk-averse*” designs.

Though the computational approach detailed is general, and can support any type of life-cycle performance metrics, the specific objectives that are considered here are the (a) expected life-cycle cost, and the (b.i) repair cost or (b.ii) repair time with specific probability of exceedance over the lifetime of the structure. Objective (a) and any of the objectives in (b) represent a set of competing objectives, and therefore a well-posed multi-objective design problem, since the former incorporates the upfront cost of the protective devices whereas the latter do not. Notes that objectives (b.i) and (b.ii) are not directly competing, so simultaneous consideration of both of them offers little additional information. Here, each of these objectives will be separately combined with objective (a) in the multi-criteria design problem formulation, resulting in a separate design problem. Since each of these objectives, (b.i) and (b.ii), represents a different measure of seismic-performance, these two design problems incorporate different practical considerations within the design formulation.

Considering as performance criteria the total life-cycle cost $C(\mathbf{x})$ and the repair cost threshold $C_{thresh}^{p_o}(\mathbf{x})$ with probability of being exceeded p_o over the considered life-time t_{life} leads to the following formulation for the multi-objective design problem

$$x^* = \arg \min_{x \in X} \{C(x), C_{thresh}^{p_o}(\mathbf{x})\}^T \quad \text{such that } P[L_t > C_{thresh}^{p_o}(\mathbf{x}) | x, t_{life}] = p_o \quad (6)$$

Similar formulation holds when the repair time is considered as the second objective [simply replace $C_{thresh}^{p_o}(\mathbf{x})$ in (6) by $R_{thresh}^{p_o}(\mathbf{x})$]. The design problem in (6) will be abbreviated by D_1 herein, and the alternative one, when $R_{thresh}^{p_o}(\mathbf{x})$ is substituted as objective, by D_2 . The probabilistic quantification of all these objectives has been discussed in Section 2.2. The multi-objective optimization in (6) leads to a set of points, known as dominant designs, which form a manifold in the objective space, the so-called Pareto front. A point belongs to the Pareto front and it is called Pareto optimal point if there is no other point that improves one objective without detriment to the other one. Once these Pareto fronts are established the decision-maker (e.g. building owner) can choose among a range of retrofitting solutions (Pareto optimal solutions) that describe different attitudes towards risk.

4. Multi-objective optimization supported by kriging surrogate modeling

4.1 Metamodel implementation details

The solution of the design problem requires different risk metrics whose estimation involves calculation of various probabilistic quantities as detailed in Section 2.2. These quantities are dependent upon the response vector \mathbf{z} , which includes the engineering demand parameters required for the fragilities of the different assemblies for calculation $L_f(\boldsymbol{\theta}, \mathbf{w}, \varepsilon_p | \mathbf{x})$ [or $R_f(\boldsymbol{\theta}, \mathbf{w}, \varepsilon_p | \mathbf{x})$] as well as any response quantities needed to quantify the upfront cost of the protective devices. Due to the potential complexity of the adopted numerical and probability models, relying on nonlinear time-history analysis and a comprehensive characterization of the seismic hazard, evaluation of these probabilistic quantities can be reliably performed only through stochastic simulation. This setting creates a significant computational burden for the associated design optimization [14].

For efficiently performing this optimization a kriging metamodeling approach is adopted here. The metamodel is developed in the so-called augmented input space [15], composed of both \mathbf{x} and $\boldsymbol{\theta}$ [metamodel input]. The developed metamodel can then simultaneously support the uncertainty propagation (with respect to $\boldsymbol{\theta}$) and the design optimization (with respect to \mathbf{x}), which facilitates significant computational savings. For



addressing the influence of the high-dimensional stochastic sequence \mathbf{w} , involved in the seismic hazard representation, within the metamodeling formulation the statistical approximation presented in [16] is adopted. This is facilitated by assuming that under the influence of \mathbf{w} each response quantity z_k follows a lognormal distribution with median \bar{z}_i and coefficient of variation σ_{z_k} . Under this assumption the probabilistic integral for estimating seismic risk in (1) simplifies to (influence of \mathbf{w} removed)

$$H_r(\mathbf{x}) = \int_{\Theta} \sum_{\varepsilon_p} \bar{h}_r(\boldsymbol{\theta}, \varepsilon_p | \mathbf{x}) p(\boldsymbol{\theta}) P_p(\varepsilon_p | \boldsymbol{\theta}) p(\mathbf{w}) d\boldsymbol{\theta} \quad (7)$$

with the modified risk consequence measure $\bar{h}_r(\boldsymbol{\theta}, \varepsilon_p | \mathbf{x})$ replacing the initial one $h_r(\boldsymbol{\theta}, \mathbf{w}, \varepsilon_p | \mathbf{x})$. This is ultimately established by changing any components of the different risk consequence measures that depend directly on the response vector \mathbf{z} , considering the impact of the statistical approximation for the influence of \mathbf{w} on it [16]. For the fragility in (3) or the indicator function $I_{v_{ref}}(\boldsymbol{\theta}, \mathbf{w}, \varepsilon_p | \mathbf{x})$ this modification leads to [16]

$$P[d_{kj} | z_k] \rightarrow \bar{P}_{kj}[d_{kj} | \bar{z}_k] = \Phi[\ln(\bar{z}_k / \beta_{kj}) / \sqrt{\sigma_{kj}^2 + \sigma_{z_k}^2}], \quad I_{v_{ref}}(\boldsymbol{\theta}, \mathbf{w}, \varepsilon_p | \mathbf{x}) \rightarrow \bar{h}_{v_{ref}}(\boldsymbol{\theta}, \varepsilon_p | \mathbf{x}) = \Phi[\ln(\bar{v}_D / v_{ref}) / \sigma_{v_D}] \quad (8)$$

where in the second equation \bar{v}_D and σ_{v_D} denote explicitly the median and logarithmic standard deviation, respectively, of the damper velocity v_D .

The kriging metamodel is formulated to provide predictions for the quantities needed to support evaluation of the risk consequences measures in (8), corresponding to the statistics, individual logarithmic mean and standard deviation of the responses of interest (engineering demand parameters and damper velocities), ultimately forming the n_y dimensional *metamodel output* \mathbf{y} . The n_ϕ dimensional augmented vector of both the design variables and the uncertain model parameters $\boldsymbol{\phi} = [\mathbf{x} \boldsymbol{\theta}]$ is considered as an *input vector*, whereas separate metamodels are established for the $\varepsilon_p = \text{yes}$ and $\varepsilon_p = \text{no}$ cases since these two cases ultimately represent different excitation models and different parameters comprising $\boldsymbol{\theta}$. Note that since the surrogate model is established to approximate the structural response, any components of $\boldsymbol{\theta}$ that do not influence this response, for example uncertain parameters included in the definition of $P(\varepsilon_p | \boldsymbol{\theta})$, do not need to be considered in the definition of $\boldsymbol{\phi}$.

For forming the metamodel initially, a database with n_m observations is obtained that provides information for the $\boldsymbol{\phi}$ - \mathbf{y} pair. For this purpose n_m samples for $\{\boldsymbol{\phi}^l, l=1, \dots, n_m\}$, also known as *support points*, are generated following initially a Latin hypercube grid over the expected range of values possible for each component of $\boldsymbol{\phi}$ while integrating the adaptive enhancement proposed in [16]. Stochastic ground motions are then generated according to the excitation model and the structural response is numerically evaluated. The influence of the white noise is addressed by considering n_w different samples for each $\boldsymbol{\phi}^l$ and using the statistics under these samples to ultimately quantify the response sample \mathbf{y}^l . Using this dataset the kriging model is then obtained. Details for the metamodel development may be found in [16].

4.2 Computational details for design optimization

All required probabilistic integrals for performing optimization (6) are estimated here through stochastic (Monte Carlo) simulation, ultimately utilizing the kriging model for efficient evaluation. This facilitates an accurate (since it is based on stochastic simulation) and computational efficient (since it utilizes the kriging metamodel) estimation of all required statistical quantities needed in the optimization process. Using a finite number, n_s , of samples of $\boldsymbol{\theta}$ and ε_p drawn from importance sampling densities (IS) $q(\boldsymbol{\theta} | \varepsilon_p)$ and $P_q(\varepsilon_p)$, respectively, with $\boldsymbol{\theta}^j$ and ε_p^j denoting the j^{th} sample, an approximation for the integral in (1) is given by:

$$\hat{H}_r(\mathbf{x}) = 1/n_s \sum_{j=1}^{n_s} \bar{h}_r(\boldsymbol{\theta}^j, \varepsilon_p^j | \mathbf{x}) P_p(\varepsilon_p^j | \boldsymbol{\theta}^j) p(\boldsymbol{\theta}^j) / [P_q(\varepsilon_p^j) q(\boldsymbol{\theta}^j | \varepsilon_p^j)] \quad (9)$$

The proposal densities are used to improve the efficiency of this estimation [Importance Sampling (IS)]. More details on this evaluation may be found in [4].

The design problem (6) is finally solved using an exterior sampling approach [14], utilizing the same stream of random numbers for all stochastic simulations used to calculate the different probabilistic integrals. This ultimately facilitates a consistent estimation error for all examined damper configurations, contributing to a more efficient comparison. The optimization (6) is thus transformed into a deterministic optimization problem and to obtain the Pareto front of dominant designs an elitist genetic algorithm is utilized in this study [17].



5. Illustrative application

5.1 Structural and excitation models

For the illustrative example, a three-story reinforced concrete office building with nonlinear fluid viscous dampers is considered. The dimensions of the building are 32 x 32 m and the height of each story is 4.0 m. A planar frame model with peak oriented hysteretic behavior and deteriorating stiffness and strength is utilized for the structure, modeled through the parsimonious approach detailed in [18] by representing restoring forces per floor through a nonlinear spring (exhibiting the desired hysteretic behavior). This modeling approach had been demonstrated [18] to provide seismic risk estimates with high accuracy when compared against high-fidelity numerical modeling of the structural behavior, even for moderate to large inelastic responses.

The lumped masses of all the stories are $[m_i] = [976, 932, 887]$ metric tons, $i=1,2,3$. The initial inter-story stiffnesses k_i of all stories are parameterized by $k_i = \hat{k}_i \theta_{k,i}$, $i=1,2,3$, where $[\hat{k}_i] = 789.02[1.00, 0.85, 0.70]$ MN/m are the most probable values and $\theta_{k,i}$ are nondimensional uncertain parameters, assumed to be correlated Gaussian variables. The mean value of $\theta_{k,i}$ is one and the covariance matrix corresponds to variances 0.10 for all the floors and correlation coefficients 0.5 between adjacent floors and 0.2 between the first and third floor. The yield displacement per story $\delta_{y,i}$, is treated as lognormal variable with median value 0.5% of story height and c.o.v. 10%. The structure is assumed to be modally damped. The damping ratio ζ_i for all modes are treated as perfectly correlated lognormal variables with median value 5% and c.o.v. 30%. Definition of the structural model requires additional characteristics for the hysteretic behavior [18], the post-yield stiffness coefficients a_i (ratio of pre to post yield stiffnesses), the over-strength factor γ_i (ratio of ultimate to yield strength), ductility coefficient μ_i (ratio of displacement for onset of deterioration to yield displacement) and the stiffness deterioration coefficient β_i (ratio of stiffness for strength deterioration branch to initial stiffness). These are taken to have values of 0.1, 0.2, 4, and 0.2 respectively. Detailed discussion of the numerical model is included in [4].

The retrofitting of this structure with nonlinear fluid viscous dampers is examined. The damper forces are given by $F_D = c_D \text{sgn}(v_D) |v_D|^{\alpha_D}$ where c_D is the damper coefficient, v_D is the damper velocity introduced earlier and α_D is the velocity exponent. The design variables in this problem correspond to the damper coefficients in each story $c_{D,i}$, $i = 1,2,3$. The velocity exponents for dampers α_D are taken equal to 0.5 for all dampers, corresponding to a common value for seismic applications. The design domain is considered as $[0.0 \ 9.2]$ MN/(m/sec)^{0.5} for $c_{D,1}$, $[0.0 \ 8.4]$ MN/(m/sec)^{0.5} for $c_{D,2}$, and $[0.0 \ 5.1]$ MN/(m/sec)^{0.5} for $c_{D,3}$. The upper limit for each damper is based on maximum force capacity desired at each floor [4].

Seismic events are assumed to occur following a Poisson distribution. The uncertainty in moment magnitude M is modeled by the Gutenberg-Richter relationship truncated on the interval $[M_{min}, M_{max}] = [5.0, 8.0]$, leading to the PDF and expected number of events per year given, respectively, by

$$p(M) = b_M \exp(-b_M M) / [\exp(-b_M M_{min}) - \exp(-b_M M_{max})], \quad v = \exp(a - b_M M_{min}) - \exp(a - b_M M_{max}) \quad (10)$$

For the regional seismicity factors, the values adopted are $a=4.35 \log_e(10)$ and $b_M=1.0 \log_e(10)$, leading to $v = 0.22$. Regarding the uncertainty in the event location and orientation with respect to the fault, the closest distance to the fault rupture, r , for the earthquake events is assumed to follow a log-normal distribution with median value $r_{med} = 20$ km and coefficient of variation 40%. Ultimately the group of uncertain model parameters is $\theta = [M, r, A_p, T_p, \gamma_p, v_p, k_i, \delta_{y,i}, \zeta]$.

5.2 Cost characteristics

The upfront damper cost $C_i(\phi)$ is estimated based on the maximum force capacity $F_{Du,i}$, as $C_{i,i} = \$ (96.88 (F_{Du,i})^{0.607})$ [4]. The ultimate damper force for each device is taken as the force with 2% probability of exceedance over the lifetime of the analysis t_{life} , calculated through estimation of an appropriate reference velocity as detailed in Section 2.2. The lifetime for the analysis t_{life} is taken as 60 years and the discount rate as 2.5%. The fragility and repair cost/repair time characteristics are reviewed in Table 1, where n_{el} corresponds to the number of elements that belong to each damageable assembly for each floor. For structural components and partitions, the maximum interstory drift is used as the engineering demand parameter (EDP), while for the rest the maximum story absolute acceleration. Detailed discussion for the adopted fragility functions and the repair



cost may be found in [4]. The repair time follows the recommendations in [12], adjusted to correspond to labor time needed to complete the work assuming one worker per 500 ft² and one worker per 1000 ft² for structural and non-structural components, respectively, following the guidelines in [19]. It should be stressed that the total repair time calculated here corresponds to the total effort, or equivalently to the repair time assuming that all necessary repairs per floor and per damageable assembly are performed in a serial manner. This of course is simply a conservative upper bound estimate for the actual total repair-downtime of the structure since jobs will proceed in parallel [1].

Table 1 – Characteristics of fragility curves and expected repair cost and time for each story.

<i>Damage state</i>	EDP	β_{kj}	σ_{kj}	n_{el}^{++}	C_{kj} (\$/n _{el})	R_{kj} (days/n _{el})
Structural components						
1 (light)	IDR ⁺	$1.0\delta_y^*$	0.20	32	2700	0.074
2 (moderate)	IDR	$(\delta_y + \delta_p^*)/2$	0.35	32	12995	0.163
3 (significant)	IDR	δ_p	0.40	32	24570	0.263
4 (severe)	IDR	δ_u^*	0.40	32	29160	0.323
5 (collapse)	IDR	5%	0.50	32	46305	27.000
Contents						
1 (damage)	PFA ⁺	0.70g	0.30	75	1500	N/A
Partitions						
1 (small cracks)	IDR	0.21%	0.60	2000 m ²	22.30	0.010
2 (moderate cracks)	IDR	0.71%	0.45	2000 m ²	60.30	0.024
3 (severe damage)	IDR	1.2%	0.45	2000 m ²	92.70	0.038
Ceiling						
1 (some tiles fallen)	PFA	0.55g	0.40	648 m ²	15.20	0.08
2 (extensive tile fallout)	PFA	1.00g	0.40	648 m ²	120.10	0.056
3 (total ceiling collapse)	PFA	1.50g	0.40	648 m ²	237.70	0.109

⁺IDR: Peak interstory drift; PFA: Peak floor acceleration

⁺⁺ n_{el} : number of elements per story

* δ_y yield displacement, δ_p displacement at maximum strength, δ_u displacement at onset of stiffness degradation

5.3 Development of surrogate model and optimization details

Separate metamodels are established for ground motions with, i.e. $\varepsilon_p = yes$, or without, i.e. $\varepsilon_p = no$, pulses. The augmented input vector ϕ is composed of \mathbf{x} as well as the components of θ that are essential for estimating the structural response, and it corresponds to $\phi = [c_{D,i}, M, r_{rup}, A_p, T_p, \gamma_p, v_p, \theta_{k,i}, \delta_{y,i}, \zeta; i=1, \dots, 3]$ ($n_\phi=16$ parameters) and $\phi = [c_{D,i}, M, r_{rup}, \theta_{k,i}, \delta_{y,i}, \zeta; i=1, \dots, 3]$ ($n_\phi=16$ parameters), for $\varepsilon_p=yes$ and $\varepsilon_p=no$ excitations, respectively. A total of $n_m=6000$ support points is used and the influence of the white noise is addressed by considering $n_w=100$ samples. The response quantities predicted from the metamodel correspond to the peak interstory drifts, peak floor accelerations and peak damper velocities for the three stories of the structure. The accuracy of the developed surrogate model is evaluated by calculating different error statistics using the leave-one-out cross-validation approach. The accuracy established is ultimately high with coefficient of determination over 97% and mean error less than 5% for most approximated response quantities. The optimized kriging metamodels are then utilized to support the design optimization. For the stochastic simulation a total of $n_s = 10000$ samples are used with properly selected importance sampling densities for key parameters, M , r_{rup} and ε_p , as in [4]. The multi-objective optimization identifies a large, complete set of Pareto optimal solutions but to simplify the presentation of the results here, a representative set of points, providing a balanced distribution along the Pareto front, is used to describe each Pareto curve.

5.4 Results and discussion

Three different values are examined for $p_o=1, 5, 10\%$. The performance for the unretrofitted structure (without the dampers) is $C=1.74$ (\$10⁵) for the total cost and $C_{thresh}=9.20, 5.99, 4.31$ (\$10⁵) and $R_{thresh}=154.77, 113.97, 92.31$ days for repair cost and repair time thresholds, respectively, for the three different p_o values 1, 5 and 10%.



For the structure with the fluid viscous dampers, Fig. 2 presents the Pareto curve for design problem D_1 (when $C_{thresh}(\mathbf{x})$ is considered as the secondary objective) [part (a)] as well as for design problem D_2 (when $R_{thresh}(\mathbf{x})$ is considered as the secondary objective) [part(b)]. For each curve the *risk neutral* ($[C_{min}, C_{thresh,max}^{p_o}]$ for D_1 and $[C_{min}, R_{thresh,max}^{p_o}]$ for D_2) and *risk-averse* ($[C_{max}^{p_o}, C_{thresh,min}^{p_o}]$ for D_1 and $[C_{max}^{p_o}, R_{thresh,min}^{p_o}]$ for D_2) designs are distinguished. In addition, a *balanced* design ($[C_m^{p_o}, C_{thresh,m}^{p_o}]$ for D_1 and $[C_m^{p_o}, R_{thresh,m}^{p_o}]$ for D_2) is identified, representing a solution in the middle of the Pareto front. Comparisons of the curves in Fig. 2 to the values for the unretrofitted structure reported previously shows the efficiency established through the seismic retrofitting, as well as the versatility of offering a range of solutions with a different compromise between the chosen objectives. This also validates the computational efficiency of the proposed framework; once the surrogate model is established, it can be utilized to support the optimization for different objectives (design problems D_1 or D_2 here) as well as for different values of p_o . The identified Pareto fronts demonstrate a significant variability for the different objectives and ultimately allow the stakeholder to examine in detail the compromise offered by different solutions in converging to a final decision. In aiding this decision additional features of the life-cycle performance can be examined, like the decomposition of the total or repair cost to their different components.

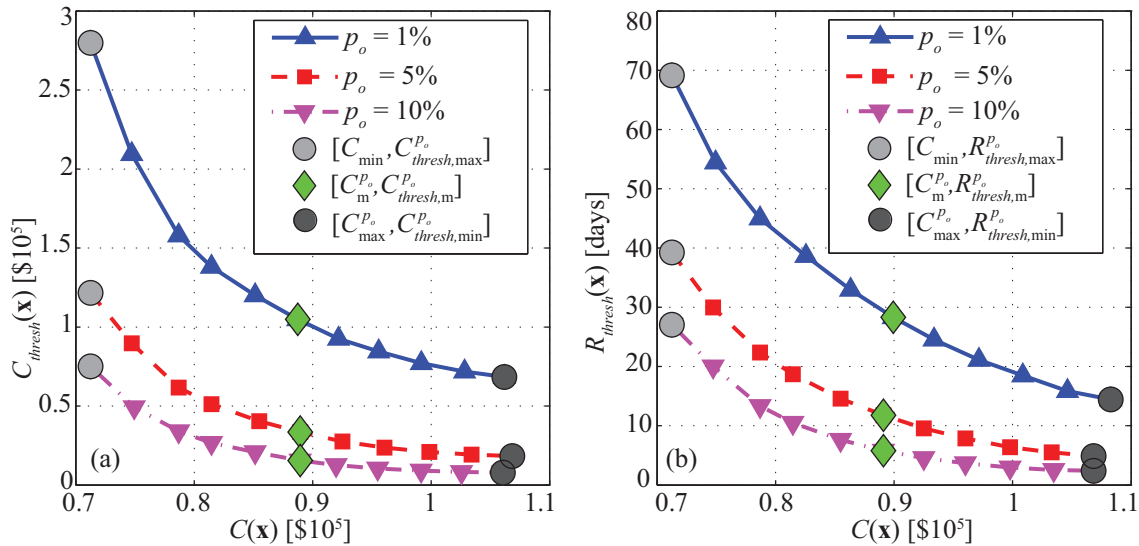


Fig. 2 – Pareto front curves for different probabilities of exceedance p_o for design problem (a) D_1 and (b) D_2 .

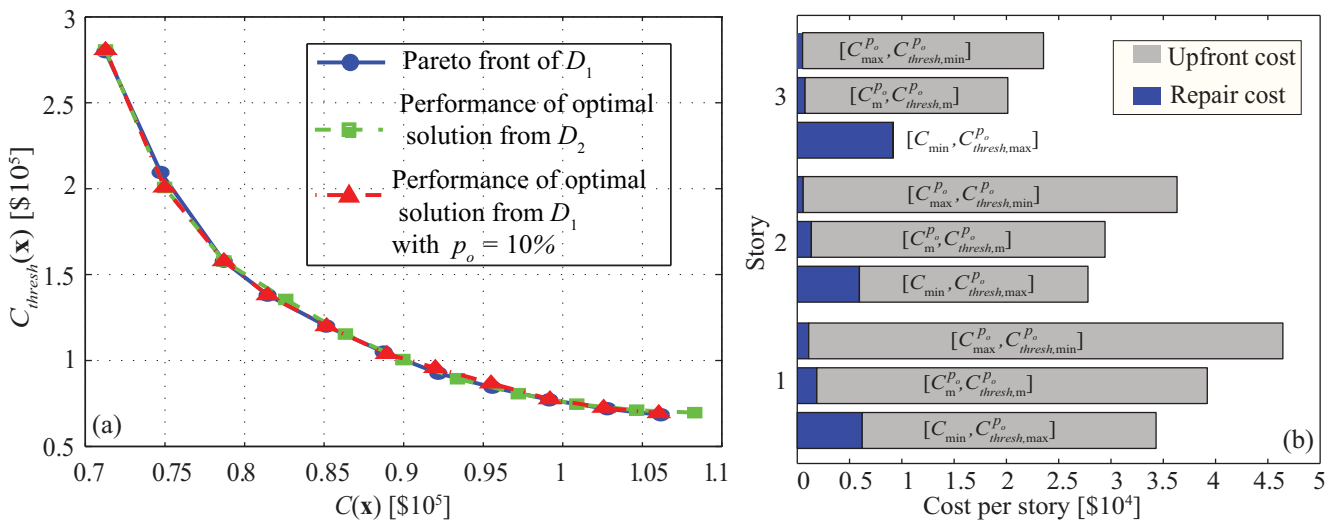


Fig. 3 – (a) Comparison of performance attained for objective space for design problem D_1 for $p_o=1\%$ for designs established under different criteria and (b) distribution of life-cycle cost between different stories for the three reference Pareto optimal designs corresponding to design problem D_1 and $p_o=1\%$.

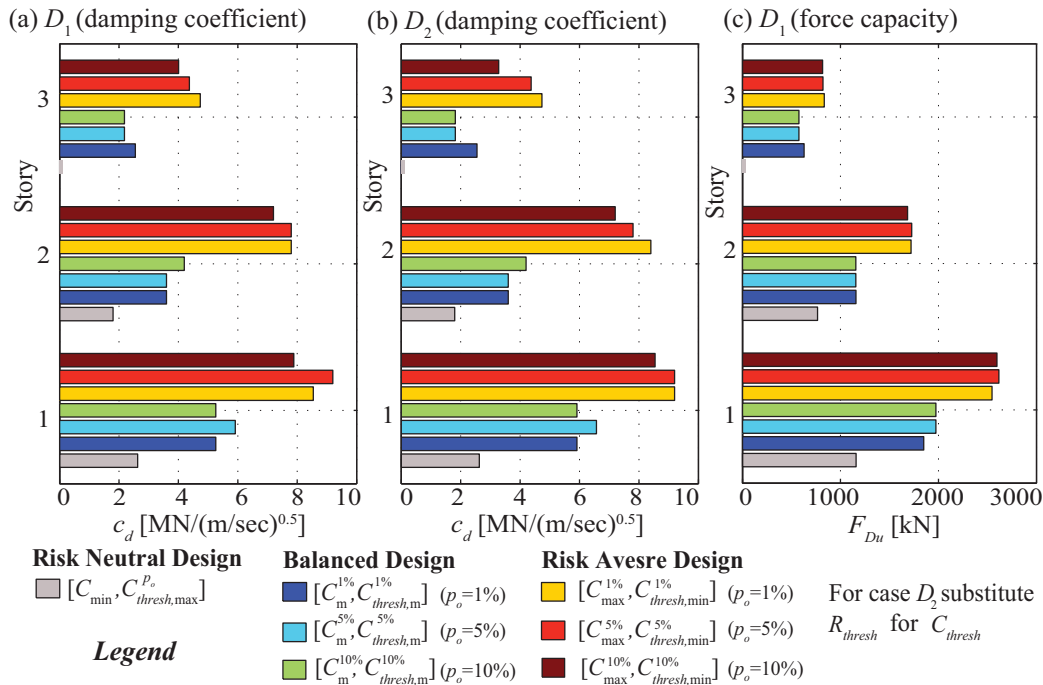


Fig. 4 – Damping coefficients of different reference Pareto optimal configurations for design problem D_1 [part (a)] and D_2 [part (b)], and corresponding maximum damper capacity for design problem D_1 [part (c)].

Fig. 3 (a) presents a comparison of the performance established by utilizing different criteria, examining how the secondary objective (i.e. choice of C_{thresh} or R_{thresh}) as well as the value of p_o impact the design. This is established by presenting the performance in the objective space corresponding to problem D_1 and value of $p_o=1\%$ for three different cases: the respective Pareto-front for that design case, the optimal solution from D_2 for $p_o=1\%$, as well as the optimal solution from D_1 for $p_o=10\%$. This comparison shows that design D_2 accomplishes only a slightly inferior performance than the actual Pareto front (design D_2). The agreement of the curves validates the similarity, argued earlier, of the secondary design objectives. The comparison between the performance established for $p_o=1\%$ and $p_o=10\%$ also shows a practically identical performance. This result indicates that the selection of value of p_o , at least for the cases examined here, does not significantly alter the design performance. Then in Fig. 3 (b) the distribution of the life-cycle cost between the different stories is shown for the characteristic Pareto optimal designs that correspond to design D_1 and $p_o=1\%$. Additionally, the decomposition of the life-cycle cost per story to upfront and repair cost is presented. It is interesting to note that while the damper cost decreases when moving to higher stories, the distribution of the repair losses along the height of the structure is more regular. This trend is attributed to the fact that for all the Pareto optimal designs the damping coefficients are higher in the lower floors (see also Fig. 4 next) as a result of the higher seismic shear forces acting on these floors; hence earthquake damages are reduced to greater extent.

Fig. 4 reports the optimal damper configuration (distribution of dampers along height of structure) with respect to the damping coefficient for design problems D_1 [part(a)] and D_2 [part(b)] and with respect to the maximum force capacity for design problem D_1 [part(c)]. Overall, the results show that the various characteristic Pareto optimal solutions lead to significantly different configuration designs (Fig. 4), which consequently result to different levels and distributions of expected costs (Fig. 2). For example if the *risk-averse* design $[C_{max}^{p_o}, C_{thresh,min}^{p_o}]$ (or $[C_{max}^{p_o}, R_{thresh,min}^{p_o}]$) is preferred then the repair cost threshold $C_{thresh}^{p_o}$ is minimized leading to negligible structural damages and minimal damages to partitions, whereas the contribution of the acceleration sensitive components prevails (nonlinear damper can suppress displacement quantities more efficiently than acceleration quantities). However, the latter design is achieved with the expense of using big dampers associated with a significantly high upfront damper cost $C_f(\mathbf{x})$ corresponding to 98% of the total life-cycle cost C . On the other hand, if a less conservative design is chosen ($[C_m^{p_o}, C_{thresh,m}^{p_o}]$ or $[C_m^{p_o}, R_{thresh,m}^{p_o}]$) then the reduction in C is 19%, with the trade-off of a 52% increase in $C_{thresh}^{p_o}$ (or 93% increase in $R_{thresh}^{p_o}$ for D_2). The *risk-neutral* design leads



to the minimum total life-cycle cost C (reduction of 33% over *risk-averse* design), establishing in this case a balance between repair C_l and upfront cost C_i , with the latter contributing only 70% towards C . However, this design approach does not explicitly suppress response for low likelihood but for large consequence events, leading to a very high value of $C_{thresh}^{p_o}$ (or equivalently $R_{thresh}^{p_o}$ for D_2 problem), an increase of around 300%. Finally Fig. 5 demonstrates the decomposition across the Pareto-front of the different cost components. This is established by showing the variation as a function of the total cost C of the percentage (%) contribution of the upfront cost (with respect to the total cost) and the percentage (%) contribution of the structural components, partitions, contents and ceiling (with respect to the repair cost). The results show that the damper upfront cost dominates the total life-cycle cost (large values of C_i/C) while it rapidly increases as the formulation moves from risk-neutral to risk-averse concepts, moving quickly towards a plateau. For the contribution of the different damageable assemblies to the repair cost (i.e. C_{str}/C_l , C_{part}/C_l , C_{cont}/C_l and C_{ceil}/C_l curves), as the size of the dampers increases (move towards risk-averse designs) the contribution from structural contents becomes quickly zero whereas the contribution from damages in partitions also decreases.

Overall the discussions here show that the retrofitting scheme with fluid viscous dampers leads to significant improvement in performance, that the risk-informed design facilitates a clear characterization of this improvement, and that the multi-objective formulation supports the identification of a range of solutions, allowing stakeholders to incorporate their own preferences (and risk aversion attitude) in the final decision.

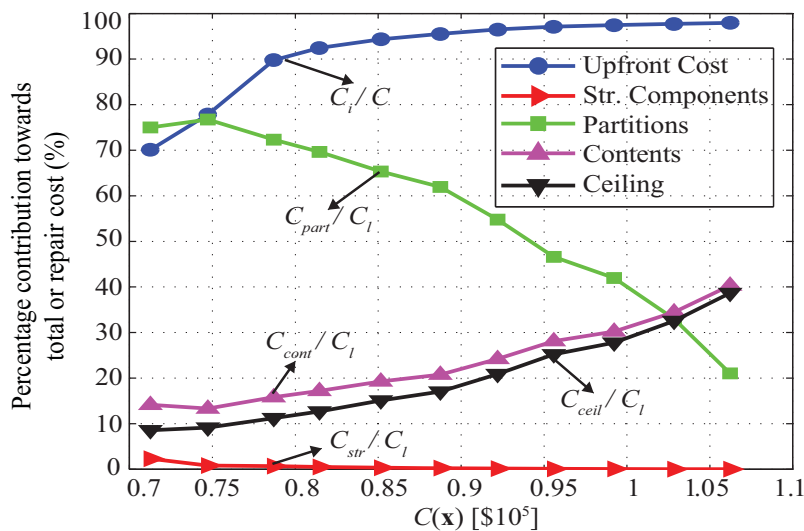


Fig. 5 – Variation across the Pareto optimal points of contribution of the different cost components, upfront cost with respect to total cost C_i/C and structural components C_{str}/C_l , partitions C_{part}/C_l , contents C_{cont}/C_l and ceiling C_{ceil}/C_l with respect to repair cost. Case plotted corresponds to design problem D_1 and $p_o=1\%$.

6. Conclusions

The multi-objective design of supplemental seismic protective devices considering life-cycle cost criteria was discussed in this paper, focusing on application to fluid viscous dampers. The fundamental metric examined as design objective is the total life-cycle cost with additional (secondary) metrics corresponding to performance quantities, repair costs or repair time in this study, with specific probability of exceedance over the life-cycle of the structure. A modeling/computational framework was discussed based on an assembly-based vulnerability approach for estimation of seismic losses and characterizing the earthquake hazard through a stochastic ground motion model. For the efficient optimization a kriging surrogate model was developed to approximate the structural response with respect to both the damper configuration and the uncertain model parameters. The development of this model involves a considerable upfront computational burden for evaluating the system response for an ensemble of ground motions, but ultimately facilitates a highly accurate and efficient approximation to the various engineering demand parameters needed for estimating the probabilistic performance, and therefore an efficient design optimization. The examined example illustrated that the multi-



objective formulation of the optimization problem offers the flexibility of considering retrofitting schemes associated with various decision-making preferences towards risk, ranging from *risk-neutral* attitude to *risk-averse* attitude. Close agreement was reported, as expected for the additional (secondary) objectives, i.e. considering repair cost or repair time thresholds. Despite this agreement, the ability to consider any of the two showcases the versatility of the established approach, as it is capable of supporting the estimation of diverse design goals. Overall the discussion showcased the enhanced risk and design information that the multi-criteria approach can offer, something exceptionally important for designing advanced seismic protective devices.

7. References

- [1] Goulet CA, Haselton CB, Mitrani-Reiser J, Beck JL, Deierlein G, Porter KA, Stewart JP (2007) Evaluation of the seismic performance of code-conforming reinforced-concrete frame building-From seismic hazard to collapse safety and economic losses. *Earthquake Engineering and Structural Dynamics*, **36** (13), 1973-1997.
- [2] Liu M, Burns SA, Wen YK (2003) Optimal seismic design of steel frame buildings based on life cycle cost considerations. *Earthquake Engineering and Structural Dynamics*, **32**, 1313-1332.
- [3] Shin H, Singh MP (2014) Minimum failure cost-based energy dissipation system designs for buildings in three seismic regions Part II: Application to viscous dampers. *Engineering Structures*, **74**, 275-282.
- [4] Gidaris I, Taflanidis AA (2015) Performance assessment and optimization of fluid viscous dampers through life-cycle cost criteria and comparison to alternative design approaches. *Bulletin of Earthquake Engineering*, **13** (4), 1003-1028.
- [5] Lavan O, Dargush GF (2009) Multi-objective evolutionary seismic design with passive energy dissipation systems. *Journal of Earthquake Engineering*, **13** (6), 758-790.
- [6] Bucher C (2009) Probability-based optimal design of friction-based seismic isolation devices. *Structural Safety*, **31** (6), 500-507.
- [7] Cha EJ, Ellingwood BR (2014) Seismic risk mitigation of building structures: The role of risk aversion. *Structural Safety*, **40**, 11-19.
- [8] Haukaas T (2008) Unified reliability and design optimization for earthquake engineering. *Probabilistic Engineering Mechanics*, **23** (4), 471-481.
- [9] Boore DM (2003) Simulation of ground motion using the stochastic method. *Pure and Applied Geophysics*, **160**, 635-676.
- [10] Mavroeidis GP, Papageorgiou AS (2003) A mathematical representation of near-fault ground motions. *Bulletin of the Seismological Society of America*, **93** (3), 1099-1131.
- [11] Christopoulos C, Filiatrault A (2006): *Principles of passive supplemental damping and seismic isolation*. Pavia, Italy: IUSS Press.
- [12] FEMA-P-58 (2012): *Seismic performance assessment of buildings*. Redwood City, CA. American Technology Council.
- [13] Taflanidis AA, Beck JL (2009) Life-cycle cost optimal design of passive dissipative devices. *Structural Safety*, **31** (6), 508-522.
- [14] Taflanidis AA, Beck JL (2008) An efficient framework for optimal robust stochastic system design using stochastic simulation. *Computer Methods in Applied Mechanics and Engineering*, **198** (1), 88-101.
- [15] Taflanidis AA, Medina JC (2014): Adaptive kriging for simulation-based design under uncertainty: Development of metamodels in augmented input space and adaptive tuning of their characteristics. *SIMULTECH 2014: 4th International Conference on Simulation and Modeling Methodologies, Technologies and Applications*, 28-30 August Vienna, Austria.
- [16] Gidaris I, Taflanidis AA, Mavroeidis GP (2015) Kriging metamodeling in seismic risk assessment based on stochastic ground motion models. *Earthquake Engineering & Structural Dynamics*, **44** (14), 2377-2399.
- [17] Kalyanmoy D (2001): *Multi-Objective Optimization using Evolutionary Algorithms*: John Wiley & Sons.
- [18] Gidaris I, Taflanidis AA (2013) Parsimonious modeling of hysteretic structural response in earthquake engineering: Calibration/validation and implementation in probabilistic risk assessment. *Engineering Structures*, **49**, 1017-1033.
- [19] Hutt CM, Almufti I, Willford M, Deierlein G (2015) Seismic Loss and Downtime Assessment of Existing Tall Steel-Framed Buildings and Strategies for Increased Resilience. *Journal of Structural Engineering*, doi 10.1061/(ASCE)ST.1943-541X.0001314, C4015005.